Geological Magazine

www.cambridge.org/geo

The origin of the ultrahigh-pressure Tso Morari complex, NW Himalaya: implication for early Paleozoic rifting

Takeshi Imayama[1], Dripta Dutta[1,2] and Keewook Yi[3]

[1]Research Institute of Frontier Science and Technology, Okayama University of Science, Okayama, Japan; [2]Department of Earth Sciences, Indian Institute of Technology Kanpur, Kanpur, UP, India and [3]Geochronology Team, Korea Basic Science Institute, Ochang, Republic of Korea

Original Article

Cite this article: Imayama T, Dutta D, and Yi K. The origin of the ultrahigh-pressure Tso Morari complex, NW Himalaya: implication for early Paleozoic rifting. *Geological Magazine* https://doi.org/10.1017/S0016756824000025

Received: 6 June 2023
Revised: 5 January 2024
Accepted: 8 January 2024

Keywords:
Ultrahigh-pressure eclogite; Ladakh Himalaya; trace element geochemistry; U–Pb SHRIMP dating

Corresponding author:
T. Imayama; Email: imayama@ous.ac.jp

Abstract

The origins and age distribution of the Himalayan high-pressure (HP) and ultrahigh-pressure (UHP) metamorphic rocks are critical for understanding the pre-Himalayan history. Although the protoliths to the UHP Tso Morari eclogites in Ladakh, NW Himalaya are believed to be the Permian Panjal volcanics, the geochronological evidence is absent. Here, we demonstrate that the protoliths of the UHP Tso Morari Complex formed in a continental rift setting at the Indian margin associated with the northern East Gondwana during the Early Paleozoic. Zircon U–Pb dates from eight gneisses and one garnet amphibolite indicate the Early Paleozoic bimodal magmatism of 493–476 Ma, which could be associated with the separation of South China from North India. Except for arc-related eclogites found in the Nidar ophiolite, the eclogites and amphibolites are rift-related, exhibiting enriched light rare earth elements and high concentrations of incompatible elements, along with evidence for crustal contamination. Our findings support the previously reported diversity in the sources and ages of the protoliths of the Himalayan HP–UHP metamorphic rocks along the orogen.

1. Introduction

High-pressure (HP) to ultrahigh-pressure (UHP) metamorphic rocks such as the eclogites are ubiquitous at the zones of oceanic plate subduction and continental collision in orogenic belts. They provide important geodynamic constraints on the regional tectono-metamorphic evolution. Numerous HP and UHP metamorphic rocks are present in the Tibet-Himalayan orogen and its vicinity (Fig. 1). The Himalayan eclogites can be broadly grouped as UHP coesite-bearing eclogites from the NW Himalaya (Tso Morari in Ladakh, NW India and Kaghan in NW Pakistan) (Guillot *et al.* 1997; Mukherjee & Sachan, 2001, de Sigoyer *et al.* 2004, St-Onge *et al.* 2013; Rehman *et al.* 2016) and HP eclogites from the central Himalaya Ama Drime Massif and Arun area in eastern Nepal (Lombardo & Rolfo, 2000; Groppo *et al.* 2007; Cottle *et al.* 2009; Corrie *et al.* 2010; Imayama *et al.* 2020). Previous petrological and geochronological works demonstrate that the geothermal gradient of the UHP eclogites is significantly lower than that of their HP counterparts (Kohn, 2014; O'Brien, 2019 and references therein). Although the differences in the origin of the two eclogite types have not received much attention, they are important to understand the pre-Himalayan geological history and the regional geological variations along the orogeny.

Generally, the protoliths of the UHP eclogites in the NW Himalaya are thought to have been basalts associated with the Permian Panjal Traps formed in a continental rift setting (Spencer *et al.* 1995; de Sigoyer *et al.* 2004). In the NW Himalaya, the Panjal volcanics regionally intruded into the High-Tethyan Himalayas (Shellnutt, 2016). The Kaghan eclogites (259±10 Ma) and associated gneisses in NW Pakistan are Early Permian in age (Rehman *et al.* 2016). The Tso Morari eclogites and associated amphibolites also exhibit geochemical signatures of a rift environment (Rao & Rai, 2006; Jonnalagadda *et al.* 2019). On the other hand, recent Nd-Sr isotope data (Ahmad *et al.* 2022) proposed their origin of ca. 289 Ma depleted Panjal volcanics and ca. 140 Ma Ladakh (Nidar) ophiolitic mafic rocks instead of the previously accepted origin from the enriched Panjal (ca. 289 Ma) and Phe volcanics (Zanskar). However, the only pre-Himalayan ages of ca. 479 Ma in the Tso Morari Crystallines (TMC) are reported for the undeformed Polokongka La granite and gneiss (Girard & Bussy, 1999), and the lack of geochronological study hinders our understanding of the origin of the UHP metamorphic rocks in the TMC. Here, we present the whole-rock geochemical analyses and zircon SHRIMP dating of the TMC gneisses and metabasites including eclogites. Our new data indicate that the UHP TMC formed in a continental rift setting during the Early Paleozoic. The results also demonstrate the diversity in the sources and ages of the HP-UHP Himalayan eclogites along the E-W direction of the orogen.

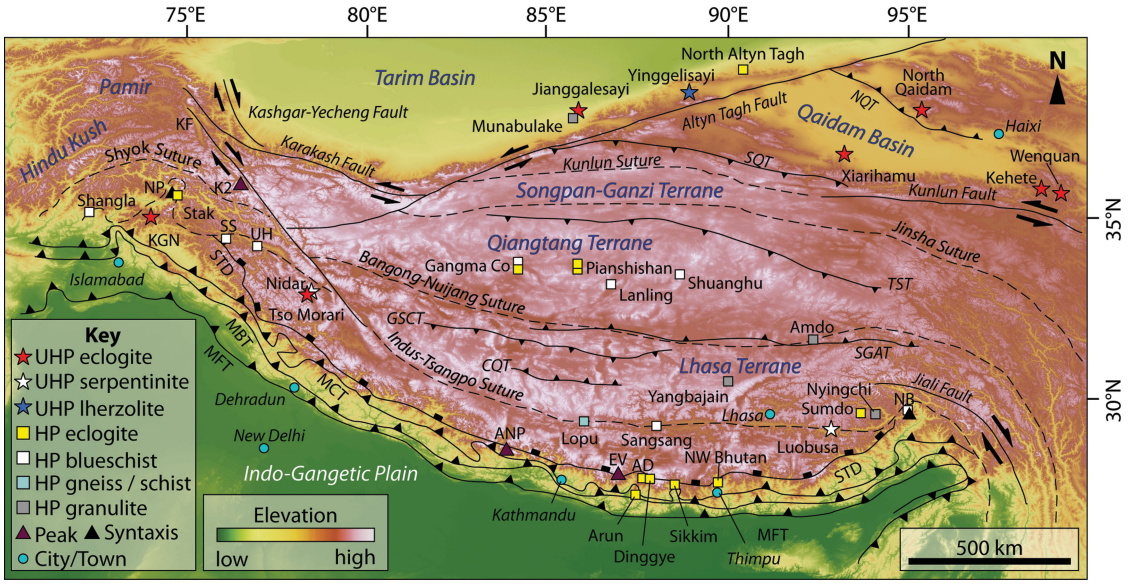

Figure 1. (Colour online) Topographic map (90 m SRTM SEM data) of the Himalaya-Tibet region illustrating the distributions of the HP-UHP metamorphic rocks (compiled from Zhang *et al.* 2005, 2014; Liou *et al.* 2009; Yang *et al.* 2009; Laskowski *et al.* 2016; Liang *et al.* 2017; Liu *et al.* 2018, 2022; Song *et al.* 2018; O'Brien, 2019; Rehman, 2019). The major discontinuities (after Li *et al.* 2015) and mountain peaks are also shown. Abbreviations *(arranged alphabetically)*: AD – Ama Drime, ANP – Annapurna, CQT – Coqin Thrust, EV – Everest, GSCT – Gaize-Siling Co Thrust, KF – Karakoram fault, KGN – Kaghan, MBT – Main Boundary Thrust, MCT – Main Central Thrust, MFT – Main Frontal Thrust, NB – Namche Barwa, NP – Nanga Parbat, NQT – Northern Qaidam Thrust, SGAT – Shinquanhe-Gaize-Amdo Thrust, SQT – Southern Qiadam Thrust, SS – Sap-Shergole, STD – South Tibetan Detachment, TST – Tanggula Shan Thrust and UH – Ursi-Hinju.

2. Geological setting

The TMC is located in the northwestern part of Indian Trans-Himalaya and is characterised by a sub-elliptical outline (Fig. 2a). It occurs as a northwesterly trending antiformal dome, separated from the Indus-Tsangpo suture including the Nidar ophiolite to the north and the Tetraogal Nappe to the south by detachment faults that dip away from the core of the dome. Further to the south, lies the Mata Nappe, which consists of two Early Paleozoic granite intrusions viz. Rupshu (ca. 482 Ma) and Nyimaling (ca. 460 Ma) (Epard & Steck, 2008). The Tso Morari Gneiss forms the core of the TMC and is overlain by a metasedimentary sequence (Fig. 2a, (Buchs & Epard, 2019). The metabasites including eclogites occur as foliation-parallel boudins (Fig. 2b, c) within the ductilely deformed gneisses (Fig. 2d). Eclogites have been widely retrogressed to amphibolites (Fig. 2e). The tectono-thermal evolution of the TMC can be broadly classified into four stages: (i) prograde metamorphism during Neo-Tethys subduction, (ii) (U)HP metamorphism under eclogite-facies condition (>2 GPa, 500–760°C) at ca. 55 Ma, (iii) near-isothermal decompression under granulite-facies condition at the mid-crustal level at ca. 48–45 Ma, and, finally, (iv) retrograde amphibolite-facies conditions at ca. 31–29 Ma (Guillot *et al.* 1997; St-Onge *et al.* 2013; O'Brien, 2019 and references therein). The Early Eocene Indo-Eurasia collision facilitated TMC extrusion along a north-easterly dipping channel (Dutta & Mukherjee, 2021). At least three deformation phases affected the TMC during extrusion and produced the gently dipping gneissic foliations (de Sigoyer *et al.* 2004; Epard & Steck, 2008).

Gneisses and metabasites samples were collected for petrographic, geochemical and geochronogical analyses (see Supplementary Materials Table S1 for sample details). Recently, Pan *et al.* (2023) investigated the fluid evolution of the TMC since the Eocene, and they sampled a traverse from the centre of an eclogite boudin out into the host orthogneiss. In this study, we focus on the protoliths of the TMC, and thus samples were not collected from the reaction zone to avoid the effects due to the metasomatism. Quartz and calcite veins are found in the o utcrops but fist-sized samples without the veins were selected for whole-rock analyses to avoid the effect of veins. Gneisses consist mainly of Ph + Bt + Pl + Qz ± Mc ± Grt ± Zo (Fig. 2f–j, mineral abbreviations are as per Whitney & Evans, 2010). They are subdivided into Ph-Bt gneiss, Grt-Ph gneiss, Ph-rich gneiss and quartzofeldspathic gneiss depending on the modal amount of minerals and presence of garnet. Most of the gneisses are orthogneisses whereas the quartzofeldspathic gneisses may be paragneisses in part. The metabasites include (retrograded) eclogites, Grt amphibolites and K-rich metabasites. Eclogite-facies metamorphism is characterised by the mineral assemblage of Grt + Omp + Rt + Coe/Qz ± Ph ± Zo (Fig. 2k–m) with later phases of Amp + Pl ±Di. The eclogites have zoning patterns in garnets associated with prograde and peak metamorphism but compositions and textures related to metasomatism stages are rare (e.g., St-Onge *et al.* 2013). The Grt amphibolites and K-rich metabasites mainly consist of Grt + Amp + Pl + Qz + Ilm + Ttn (Fig. 2n) and Grt + Bt + Ph + Amp + Pl + Qz + Rt + Zo ± Ttn, respectively.

3. Major and trace element geochemistry

The ten metabasite samples have low SiO_2 (44.09–51.20 wt%) and MgO (5.23–9.40 wt%), high TiO_2 (1.09–3.12 wt%) relative to FeO/MgO ratio and variable alkali contents (1.61–7.21 wt%) (Supplementary Materials Table S2 and Figure S1). Unlike the retrograded eclogites and K-rich metabasites, the Grt amphibolites and eclogite boulder have low alkali contents. The analysed samples plot on the field of subalkaline basalts in the Zr/TiO_2 vs. Nb/Y diagram, and the eclogite boulder has a low Nb/Y ratio (Supplementary Materials Figure S1).

https://doi.org/10.1017/S0016756824000025 Published online by Cambridge University Press

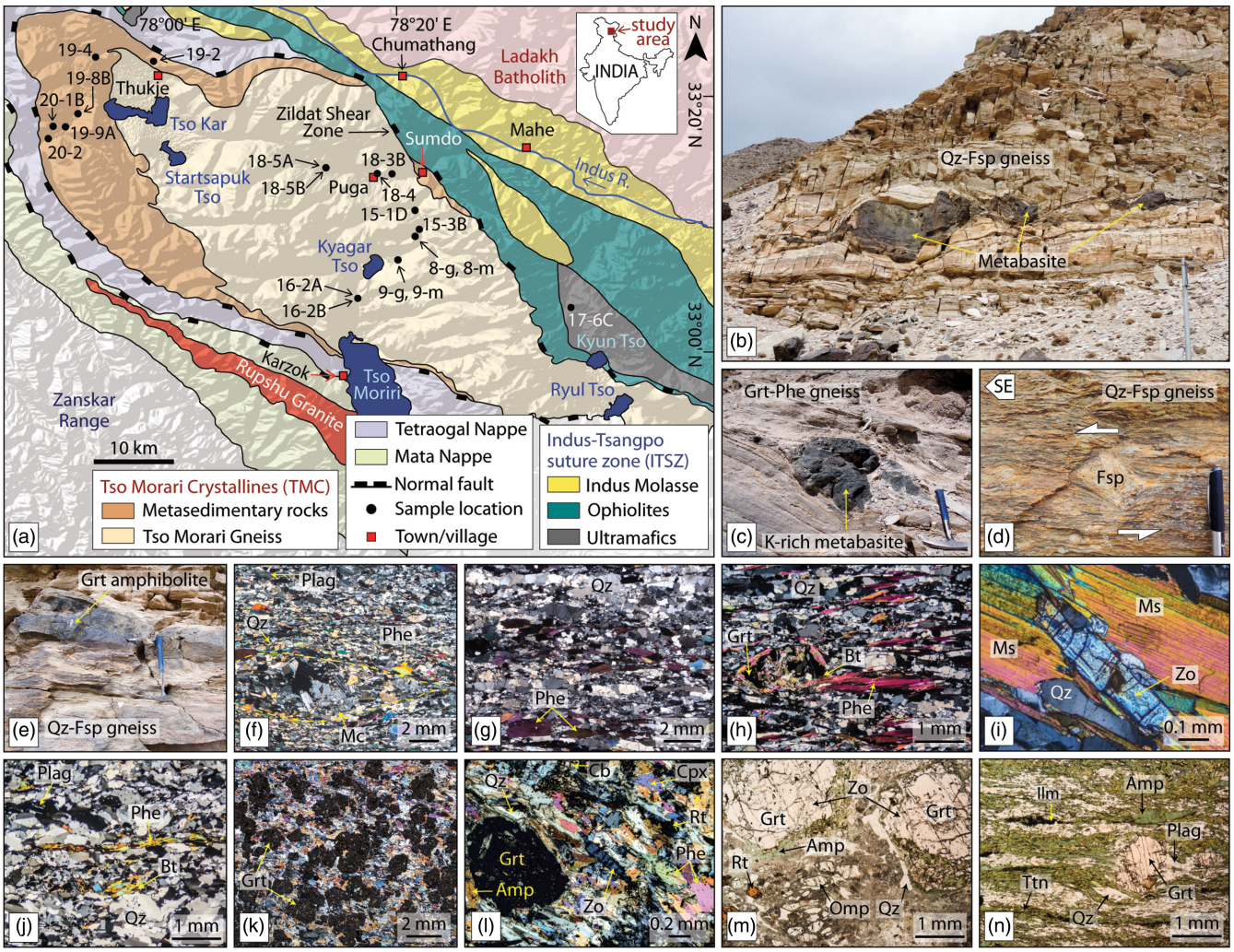

Figure 2. (Colour online) Study area, outcrop photographs and photomicrographs. (a) Geological map of the Tso Morari region (reproduced from Epard and Steck, 2008). Boudins of (b) eclogite and (c) K-rich metabasite in the Tso Morari gneiss parallel to the gneissic foliation. This photo was clicked at the same location as that of Fig. 3 by St-Onge *et al.* (2013). The large eclogite boudin is about 4 m thick at its thickest portion. (d) Top-to-the SE ductile shear sense exhibited by a feldspar augen in the quartzofeldspathic gneiss. (e) Retrograded Grt amphibolite. (f) Augen-shaped aggregates of quartz and feldspar within the fine-grained quartzofeldspathic matrix. The mica grains of the gneiss define the foliations in (g) and (h). (i) Prismatic zoisite grain within the coarser phengite grains of the gneiss. (j) Quartz porphyroclasts are common in some gneisses. Photomicrographs of the metabasites (k-m) and Grt amphibolite (n).

The large ion lithophile elements (e.g., Rb and Ba) concentrations are variable (Fig. 3a, b) due to their mobility during surface weathering and alteration processes (Xia & Li, 2019). Thus it is important to check element mobility before applying tectonic discrimination diagrams (Polat & Hofmann, 2003; Imayama *et al.* 2021). The eclogites and amphibolites lack large Ce anomalies as shown by the Ce* values between 0.96 and 1.04 ($Ce^* = Ce_N/Sqrt(La_N \times Pr_N)$), which is considered as immobile when the range is $0.9<Ce^*<1.1$. There is also no significant carbonisation or silicification due to the absence of carbonate and sulfide minerals in samples. These occurrences imply that the major chemical compositions of the sampled eclogites and amphibolites have not been strongly affected by hydrothermal alteration (Polat & Hofmann, 2003; Imayama *et al.* 2021).

All the metabasite samples are enriched in high field strength elements (HFSE) with Nb-Ta negative anomalies, and their chondrite-normalised rare earth element (REE) patterns plot in the fields between oceanic island basalt (OIB) and enriched mid-ocean ridge basalt (E-MORB, Fig. 3a–d). The HFSE and REE contents are lowest in the eclogite boulder along with prominent Nb and Zr–Hf negative anomalies. In the Nb–Zr–Y diagram, the metabasites, except for the eclogite boulder, plot in the fields of within-plate tholeiite or volcanic-arc basalts (Fig. 3e). In the Zr/Y–Zr diagram (Fig. 3f), these metabasites have high Zr/Y representing the within-plate basalts and are thus distinguished from the island-arc origin. In contrast, the eclogite boulder plots in the fields where island-arc basalt and MORB overlap on both diagrams (Fig. 3e, f).

4. Zircon U-Pb geochronology

We separated the zircons from eight gneisses and one Grt amphibolite (Fig. 2a, Supplementary Materials Table S1) to obtain cathodoluminescence (CL) images and U–Pb ages (see Supplementary Materials Text S1). The CL images of the zircon grains from the gneisses show well-developed prismatic faces and internal oscillatory zoning, which is typical igneous-type zircons

https://doi.org/10.1017/S0016756824000025 Published online by Cambridge University Press

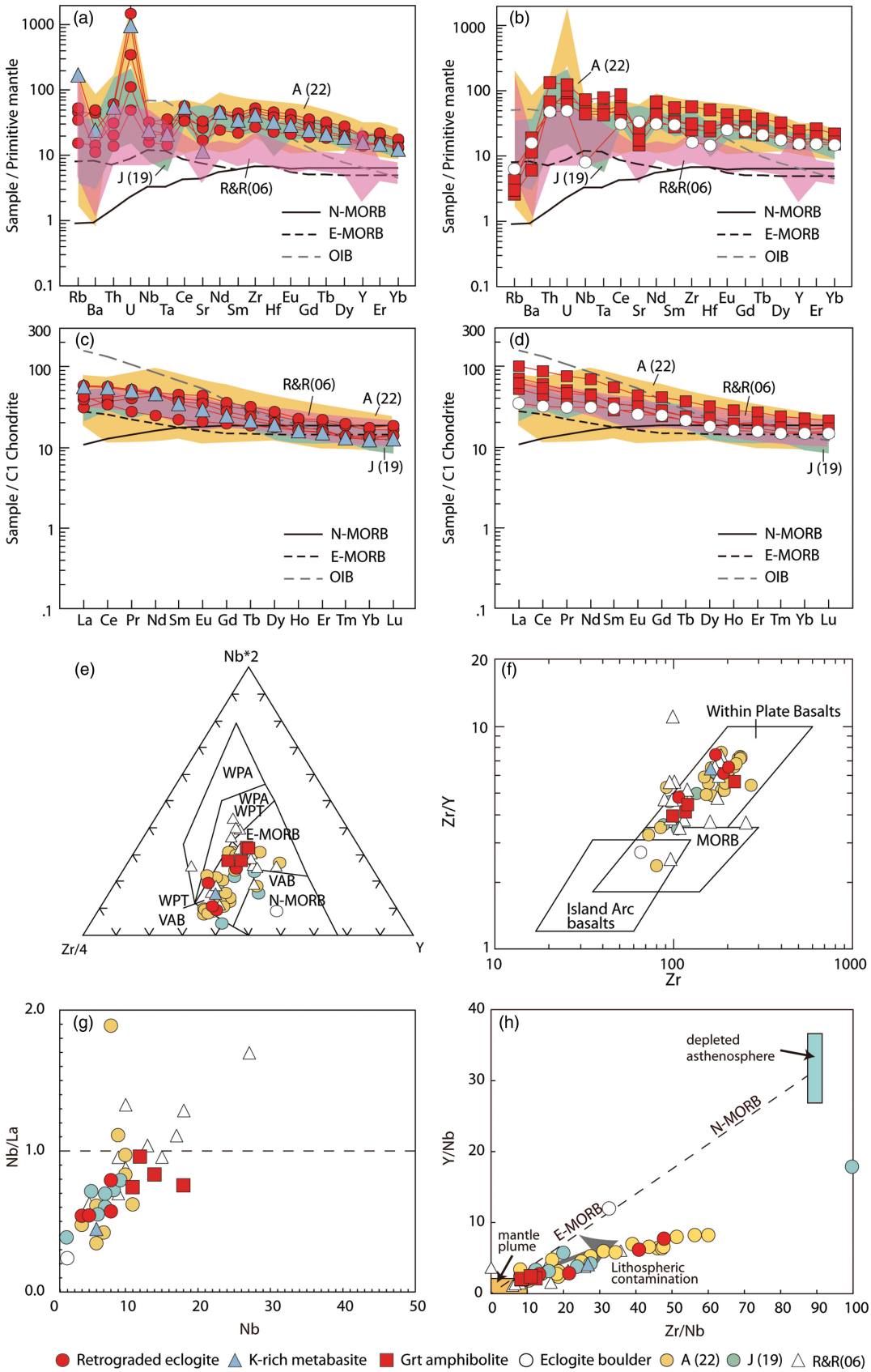

Figure 3. (Colour online) Spider diagrams of (a) retrograde eclogite and K-rich metabasite and (b) Grt amphibolite and eclogite boulder. Chondrite-normalised rare earth element patterns for (c) retrograde eclogite and K-rich metabasite and (d) Grt amphibolite and eclogite boulder. The compositions of metabasites from the TMC plotted in (e) Nb*2–Zr/4–Y (Meschede, 1986), (f) Zr/Y vs. Zr (Pearce & Norry, 1979), (g) Nb/La vs. Nb and (h) Y/Nb vs. Zr/Nb diagrams (Wilson, 1989, updated by Xia & Li, 2019). Data sources of the N-MORB, E-MORB, mantle plume and depleted asthenosphere compositions are from Sun & McDonough (1989) and Salters and Stracke (2004) with the PetDB database (http://www.earthchem.org/petdb). A(22): Ahmad *et al.* (2022), J(19): Jonnalagadda *et al.* (2019), R&R(06): Rao and Rai (2006). WPA: within-plate alkali basalts, WPT: within-plate tholeiites, VAB: volcanic-arc basalts.

https://doi.org/10.1017/S0016756824000025 Published online by Cambridge University Press

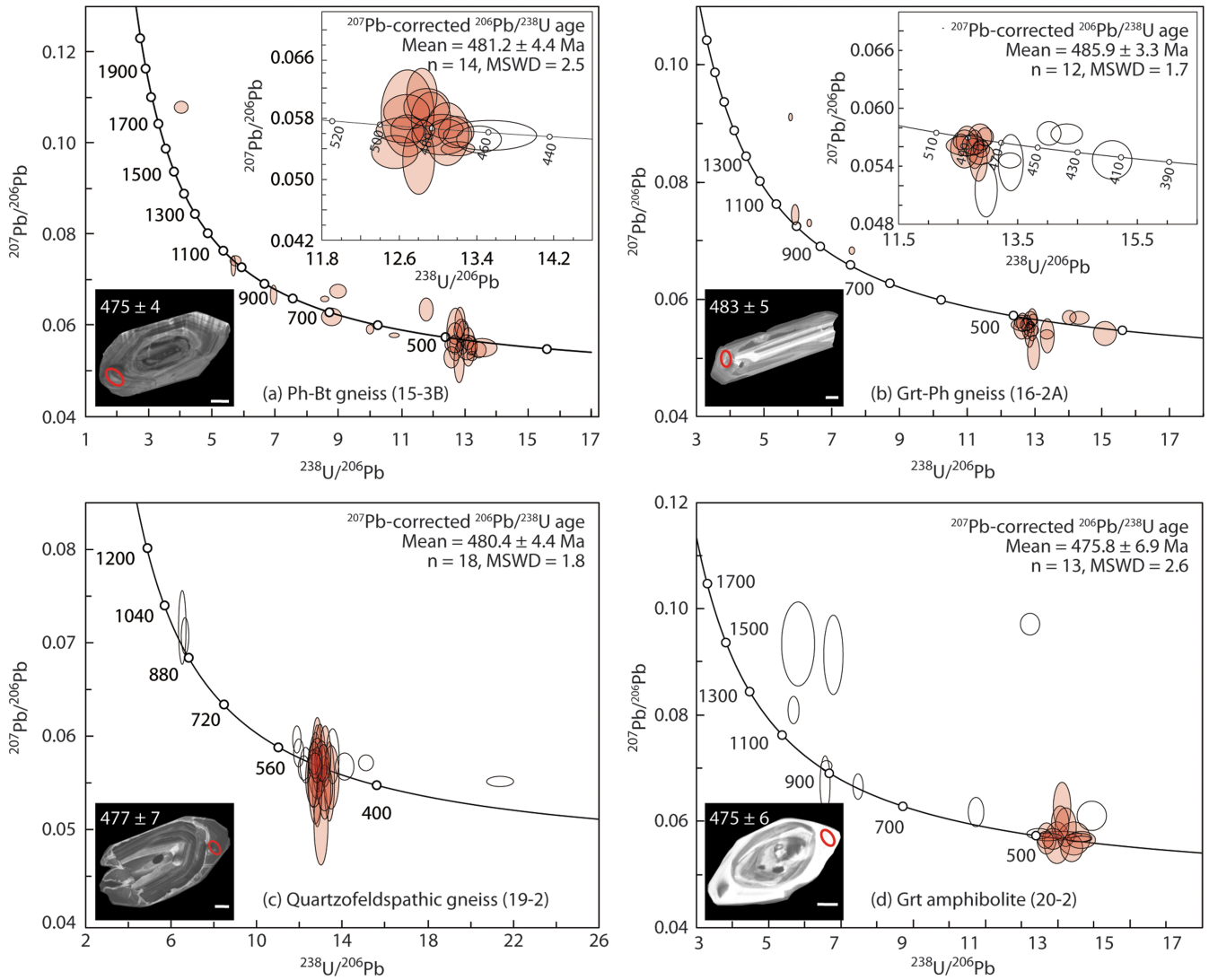

Figure 4. (Colour online) Concordia diagrams from the SHRIMP zircon U–Pb analyses of (a) Ph-Bt gneiss (15-3B), (b) Grt-Ph gneiss (16-2A), (c) Quartzofeldspathic gneiss (19-2) and (d) Grt amphibolite (20-2) from the TMC. All error ellipses and weighted mean ^{206}Pb/^{238}U ages are quoted at the 1σ and 2σ levels, respectively. The white bars below the zircons are 20 μm long.

(Fig. 4). Some grains have modified grey-CL rims showing faint oscillatory zoning or patchy pattern of dark and bright colours in CL-image (Supplementary Materials Figure S2). Thin metamorphic rims showing dark-CL domains are observed in 19-2 and 19-4, but they are too thin to analyse. The U–Pb analyses of two Ph-Bt gneisses (15-3B and 9g) concentrated at a single population of concordant to near-concordant grains with a weighted mean ^{206}Pb/^{238}U date of 481.2±4.4 Ma ($n = 14$, mean squared weighted deviation or MSWD = 2.5, Fig. 4a) and 484.3±5.7 Ma ($n = 14$, MSWD = 2.1, Supplementary Materials Figure S3a), respectively. Some grains were possibly affected by Pb-loss resulting in young ^{206}Pb/^{238}U ages. The inherited grains yielded scattered dates ranging from 1402 Ma to 606 Ma. The zircons from a Grt-Ph gneiss (18-3B) yielded ^{206}Pb/^{238}U dates ranging from 500 to 470 Ma, but the weighted mean date was not calculated due to the large MSWD value (Supplementary Materials Figure S3b). The U–Pb analyses of concordant grains from the other two Grt-Ph gneisses (16-2A and 18-4) yielded the weighted mean ^{206}Pb/^{238}U date of 485.9±3.3 Ma ($n = 12$, MSWD = 1.7, Fig. 4b) and 493.4±5.2 Ma ($n = 13$, MSWD = 1.6, Supplementary Materials Figure S3c), respectively. Some inherited grains observed in three Grt-Ph gneisses yield ^{206}Pb/^{238}U dates of 1841 to 796 Ma. The igneous zircons of 15 concordant grains from Ph-rich gneiss (18-5B) yielded the weighted mean ^{206}Pb/^{238}U date of 493.3±5.4 Ma ($n = 15$, MSWD = 2.1, Supplementary Materials Figure S3d). The inherited domains gave ^{206}Pb/^{238}U dates of 1154 to 766 Ma. Some grains from two quartzofeldspathic gneisses (19-2 and 19-4) show discordant behaviour due to the disturbance of common Pb and Pb loss. The U–Pb analyses of the crystals that yielded concordant dates gave weighted mean ^{206}Pb/^{238}U dates of 480.4±4.4 Ma ($n = 18$, MSWD = 1.8, Fig. 4c) and 485.6±4.5 Ma ($n = 14$, MSWD = 3.0, Supplementary Materials Figure S3e), respectively.

https://doi.org/10.1017/S0016756824000025 Published online by Cambridge University Press

The zircon grains from Grt amphibolite (20-2) show well-developed prismatic faces and show bright-CL oscillatory zoning surrounding the inherited core (Fig. 4d). The igneous zircons of 13 concordant grains yielded the weighted mean $^{206}Pb/^{238}U$ date of 475.8±6.9 Ma (MSWD = 2.6, Fig. 4d). The inherited domains gave $^{206}Pb/^{238}U$ dates of 1039 to 813 Ma.

5. Discussion

Previous workers suggested that the protoliths of the Tso Morari eclogites are either the Permian Panjal basalts associated with a mantle plume and crustal contamination (Spencer *et al.* 1995; de Sigoyer *et al.* 2004; Jonnalagadda *et al.* 2019) or the Late Jurassic to Early Cretaceous Ladakh ophiolitic mafic rocks in the supra-subduction zone (Ahmad *et al.* 2022). The metabasites we analysed have enriched light REE contents (Fig. 3c,d), and the mixing line for the lithospheric contamination in the Y/Nb–Zr/Nb diagram (Fig. 3h) starts from the mantle plume source, rather than the depleted MORB on the mantle array, precluding the possibility of N-MORB components in the mantle source. Although the enriched light REE patterns are comparable to both E-MORB and OIB, the concentrations of incompatible trace elements such as the HFSE are much higher than those of the E-MORB and resemble those of OIB (Fig. 3a, b). The signatures of within-plate basalts are marked by the high Zr/Y content in most metabasites (Fig. 3f). Although the Nb-Ta negative anomalies (Fig. 3a, b) and Nb/La<1 (Fig. 3g) in most of the TMC metabasites imply either continental intraplate basalts that experienced crustal contamination or island-arc basalts as their protoliths, the former is supported by high concentrations of incompatible trace elements (Xia and Li, 2019). Crustal contamination leads to low Nb content, increasing Y/Nb and Zr/Nb ratios (Fig. 3h). The trend has a different slope from that of the mantle array line from the plume, through MORB, to the depleted asthenosphere. Based on field occurrences, the contaminant lithology could partially consist of the Early Paleozoic orthogneisses surrounding metabasites. The Zr/Nb ratios from a few orthogneisses reach up to 30 (Ahmad *et al.* 2022), which exceed the average Zr/Nb ratios of around 10 for continental crust compositions (e.g., Wedepohl 1995; Rudnick & Gao, 2003). The crustal contamination is also supported by the presence of the inherited zircon cores in the garnet amphibolite (sample 20-2). Therefore, the TMC metabasites most likely formed in a continental rift setting and experienced lithospheric contamination. In contrast, the eclogite boulder with prominent Nb and Zr–Hf negative anomalies suggests its island-arc origin, which could correspond to the Nidar ophiolite mafic rocks formed by the subduction initiation in the forearc (Ahmad *et al.* 2022).

The U–Pb SHRIMP data from the eight gneisses suggest an Early Paleozoic (ca. 493–480 Ma) protolith, which is consistent with the previously reported U–Pb zircon date of 479±2 Ma from the Tso Morari Gneiss (Girard & Bussy, 1999). The youngest zircon date of 475.8±6.9 Ma was obtained from the Grt amphibolite, which represents a retrograde product of the eclogites. Oscillatory zoning is a common feature in zircons from felsic igneous rocks, but some zircon textures in amphibolites from the orogenic belts also include oscillatory zoning (Oh *et al.* 2017; Kang *et al.* 2020), representing the timing of mafic magmatism. It is unlikely that contamination of zircons from orthogneisses occurred during intrusion because the garnet amphibolite occurs within the paragneisses, not orthogneisses. The zircons may have crystalised from basaltic magmas if the rocks displayed high Zr contents (Shao *et al.* 2019). Therefore, the ca. 476 Ma zircon date from garnet amphibolite is interpreted as the timing of mafic magmatism and is roughly consistent with those of the gneisses within error, indicating the bimodal magmatism during the Early Paleozoic at least for some time. In terms of trace element geochemistry, continental basalt is similar to the OIB but the presence of coherent granites implies the tectonic setting of continental rift. These Early Paleozoic ages indicate that the TMC eclogites were not derived from the Permian Panjal Traps associated with the opening of the Neo-Tethys Ocean. The crystallisation ages (ca. 493 Ma) from the central part of the TMC near Puga are slightly older than those (ca. 486–476 Ma) in surrounding parts, implying multi-stage magmatism. Felsic rocks volumetrically dominate the TMC, whereas the volume of mafic rocks is quite small. This is also in contrast to what is observed in the NW Himalaya where the Panjal Traps are characterised by abundant mafic magmatism (Shellnutt, 2016). We alternatively propose that the protoliths of the UHP TMC formed in the extensional setting at the rifted Indian margin during the Early Paleozoic. During the Pan-African orogeny, the Indian shield was located in the northern East Gondwana (Gray *et al.* 2008, Fig. 5). Epard and Steck (2008) pointed out that the sequences deposited in the north Indian margin in the Tso Morari region are affected by extensional structures, rather than the compressional structures of the Pan-African orogeny. The Early Paleozoic tectonic events are widely known in the Himalayas (Le Fort & Cronin, 1988; Gehrels *et al.* 2006), but the investigation of the detailed tectonic evolution is beyond the scope of this study as here we only discuss the Early Paleozoic igneous events in the NW Himalaya. The report of A-type alkaline Kaghan metagranite of ca. 470 Ma (Trivedi *et al.* 1986) also supports the Early Paleozoic rifting at the passive margin of northern India. The Early Paleozoic felsic magmatism is also exposed in Pakistan (483–476 Ma, Ogasawara *et al.* 2019; ca. 459 Ma, Mughal *et al.* 2022) and in the Garhwal, NW India (495–490 Ma, Imayama *et al.* 2023; ca. 512 Ma, Sen *et al.* 2021), which are considered as S-type and A-type, respectively. Thus, the A-type Early Paleozoic granites in the Garhwal are more closely related to the Early Paleozoic rifting events in this study. Coupled with geochemical results in this study, we posit that the Early Paleozoic rifting after the Neoproterozoic Pan-African orogeny produced the protoliths of the TMC. Recently, a close relationship between North India and South China during the Neoproterozoic to Early Paleozoic has been discussed (Qi *et al.* 2020; Imayama *et al.* 2023), and the Early Paleozoic rifting in NW India led to the separation of South China from North India (Fig. 5, Imayama *et al.* 2023). However, more study is required to confirm this assumption.

Combined with the UHP Nanga Parbat eclogites (Rehman *et al.* 2016), our results suggest multiple sources and ages for the protolith of the UHP metamorphic rocks in the NW Himalaya. Similarly, the protolith of the HP metamorphic rocks in the central Himalaya also originate from multiple sources and ages (Zhang *et al.* 2022). The HP eclogites of the Ama Drime Massif originated from the Ordovician (~480–430 Ma) rift-related or E-MORB-like magmatism (Wang *et al.* 2017; Dong *et al.* 2022) and the Paleoproterozoic (~1850 Ma) continental flood basalts (Zhang *et al.* 2022). In Bhutan, the HP metabasite was derived from young Paleoproteorozoic rifting (~1742 Ma, Chakungal *et al.* 2010). These occurrences indicate the sources and ages of the protoliths of the Himalayan HP–UHP metamorphic rocks are diverse in the NW-SE direction along the orogen.

https://doi.org/10.1017/S0016756824000025 Published online by Cambridge University Press

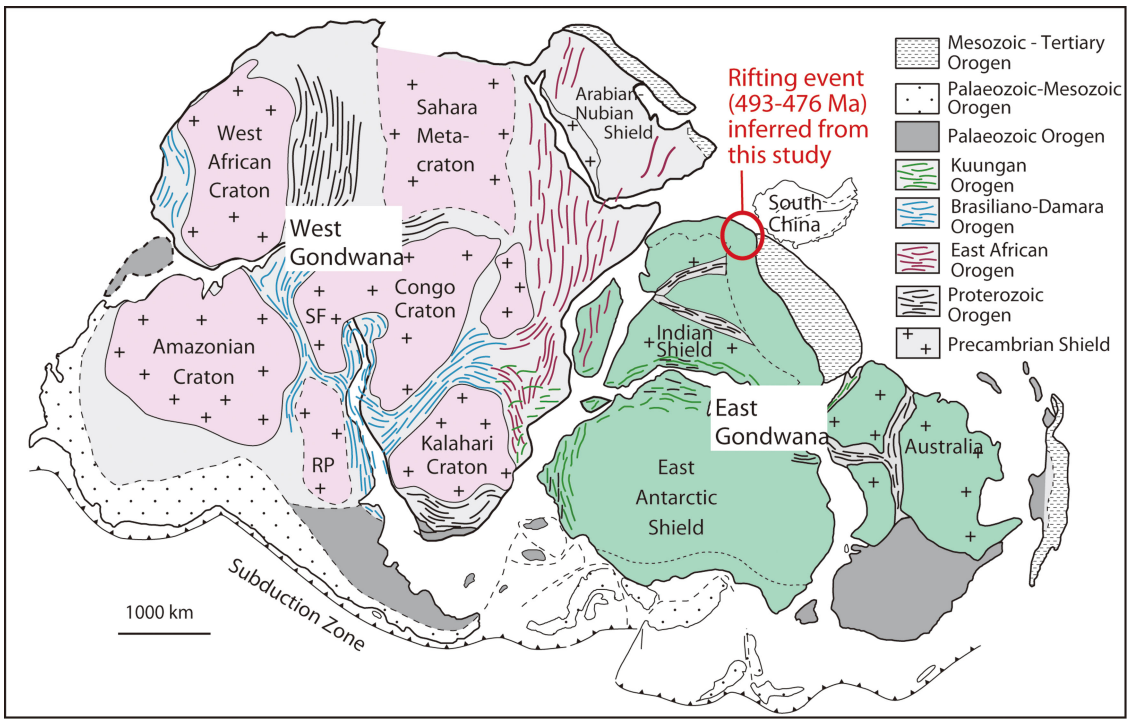

Figure 5. (Colour online) Map of Gondwana showing the positions of the Indian Shield and the rifting event inferred from this study. Modified from Gray *et al.* (2008), Meert and Lieberman (2008) and Imayama *et al.* (2023). SF, São Francisco Craton; RP, Río de la Plata Craton.

Supplementary material. To view supplementary material for this article, please visit https://doi.org/10.1017/S0016756824000025

Acknowledgements. The research was supported by the Japan Society for the Promotion of Science (22H01324) and the Korea Basic Science Institute under the R&D programme (C330430). We are grateful to Shinae Lee for the analytical work. We thank Dr. Johannes Pohlner and the anonymous reviewer for constructive and critical reviews that significantly helped to improve the manuscript. We also thank Dr. Simon Schorn for their careful editorial handling.

References

Ahmad T, Bhat IM, Tanaka T, Bickle M, Asahara Y, Chapman H and Sachan HK (2022) Tso Morari Eclogites, Eastern Ladakh: isotopic and elemental constraints on their Protolith, genesis, and tectonic setting. *The Journal of Geology* **130**, 231–52.

Buchs N and Epard J-L (2019) Geology of the eastern part of the Tso Morari nappe, the Nidar Ophiolite and the surrounding tectonic units (NW Himalaya, India). *Journal of Maps* **15**, 38–48.

Chakungal J, Dostal J, Grujic D, Duchêne S and Ghalley KS (2010) Provenance of the Greater Himalayan sequence: evidence from mafic granulites and amphibolites in NW Bhutan. *Tectonophysics* **480**, 198–212.

Corrie SL, Kohn MJ and Vervoort JD (2010) Young eclogite from the-Greater Himalayan Sequence, Arun Valley, eastern Nepal: P–T–t path and tectonic implications. *Earth and Planetary Science Letters* **289**, 406–16.

Cottle JM, Searle MP, Horstwood MSA and Waters DJ (2009) Timing of Midcrustal Metamorphism, melting, and deformation in the Mount Everest region of Southern Tibet revealed by U(-Th)-Pb geochronology. *The Journal of Geology* **117**, 643–64.

Dong X, Zhang Z, Tian Z, Niu Y and Zhang L (2022) Protoliths and metamorphism of the central Himalayan eclogites: Zircon/titanite U–Pb geochronology, Hf isotope and geochemistry. *Gondwana Research* **104**, 39–53.

Dutta D and Mukherjee S (2021) Extrusion kinematics of UHP terrane in a collisional orogen: EBSD and microstructure-based approach from the Tso Morari Crystallines (Ladakh Himalaya). *Tectonophysics* **800**, 228641.

Epard J-L and Steck A (2008) Structural development of the Tso Morari ultra-high pressure nappe of the Ladakh Himalaya. *Tectonophysics* **451**, 242–64.

Gehrels GE, DeCelles PG, Ojha TP and Upreti BN (2006) Geologic and U-Th-Pb geochronologic evidence for early Paleozoic tectonism in the Kathmandu thrust sheet, central Nepal Himalaya. *Geological Society of America Bulletin* **118**, 185–98.

Girard M and Bussy F (1999) Late Pan-African magmatism in the Himalaya: new geochronological and geochemical data from the Ordovician Tso Morari metagranites (Ladakh, NW India). *Schweizerische mineralogische und petrographische Mitteilungen* **79**, 399–418.

Gray DR, Foster DA, Meert JG, Goscombe BD, Armstrong R, Trouw RAJ and Passchier CW (2008) A Damara orogen perspective on the assembly of southwestern Gondwana. *Geological Society, London, Special Publications* **294**, 257–78.

Groppo C, Lombardo B, Rolfo F and Pertusati P (2007) Clockwise exhumation path of granulitized eclogites from the Ama Drime range (Eastern Himalayas). *Journal of Metamorphic Geology* **25**, 51–75.

Guillot S, de Sigoyer J, Lardeaux JM and Mascle G (1997) Eclogitic metasediments from the Tso Morari area (Ladakh, Himalaya): evidence for continental subduction during India-Asia convergence. *Contributions to Mineralogy and Petrology* **128**, 197–212.

Imayama T, Uehara S, Sakai H, Yagi K, Ikawa C and Yi K (2020) The absence of high-pressure metamorphism in the inverted Barrovian metamorphic sequences of the Arun area, eastern Nepal and its tectonic implication. *International Journal of Earth Sciences* **109**, 465–88.

Imayama T, Oh CW, Jeon J and Yi K (2021) Neoproterozoic and middle Paleozoic geological events in the eastern Wolhyeonri complex of the southwestern Gyeonggi Massif, South Korea, and their tectonic correlations in northeastern Asia. *Lithos* **382–383**, 105923.

Imayama T, Bose N, Yi K, Jeong Y-J, Horie K, Takehara M and Kawabata R (2023) Zircon U–Pb, Hf, and O isotopic constraints on the tectonic affinity of the basement of the Himalayan orogenic belt: insights from metasedimentary rocks, orthogneisses, and leucogranites in Garhwal, NW India. *Precambrian Research* **397**, 107183.

Jonnalagadda MK, Karmalkar NR and Duraiswami RA (2019) Geochemistry of eclogites of the Tso Morari complex, Ladakh, NW Himalayas: insights into

trace element behavior during subduction and exhumation. *Geoscience Frontiers* **10**, 811–26.

Kang W, Li W, Kang L, Dong Y, Jiang D, Liang J and Dong H (2020) Metamorphism and geochronology of garnet amphibolite from the Beishan Orogen, southern Central Asian Orogenic Belt: Constraints from P-T path and zircon U-Pb dating. *Geoscience Frontiers* **11**, 1189–201.

Kohn MJ (2014) Himalayan metamorphism and its tectonic implications. *Annual Review of Earth and Planetary Sciences* **42**, 381–419.

Laskowski AK, Kapp P, Vervoort JD and Ding L (2016) High-pressure Tethyan Himalaya rocks along the India-Asia suture zone in southern Tibet. *Lithosphere* **8**, 574–82.

Le Fort P and Cronin VS (1988) Granites in the tectonic evolution of the Himalaya, Karakoram and southern Tibet [and discussion]. *Philosophical Transactions of the Royal Society of London Series A* **326**, 281–99.

Li Y, Wang C, Dai J, Xu G, Hou Y and Li X (2015) Propagation of the deformation and growth of the Tibetan–Himalayan orogen: a review. *Earth-Science Reviews* **143**, 36–61.

Liang X, Wang G, Yang B, Ran H, Zheng Y, Du J and Li L (2017) Stepwise exhumation of the Triassic Lanling high-pressure metamorphic belt in Central Qiangtang, Tibet: insights from a coupled study of metamorphism, deformation, and geochronology. *Tectonics* **36**, 652–70.

Liou JG, Ernst WG, Zhang RY, Tsujimori T and Jahn BM (2009) Ultrahigh-pressure minerals and metamorphic terranes – the view from China. *Journal of Asian Earth Sciences* **35**, 199–231.

Liu L, Zhang J-F, Cao Y-T, Green HW, Yang W-Q, Xu H-J, Liao X-Y and Kang L (2018) Evidence of former stishovite in UHP eclogite from the South Altyn Tagh, western China. *Earth and Planetary Science Letters* **484**, 353–62.

Liu Y, Li S, Xie C, Santosh M, Liu Y, Dong Y, Wang B, Guo R and Cao X (2022) Subduction–collision and exhumation of eclogites in the Lhasa terrane, Tibet Plateau. *Gondwana Research* **102**, 394–404.

Lombardo B and Rolfo F (2000) Two contrasting eclogite types in the Himalayas: implications for the Himalayan orogeny. *Journal of Geodynamics* **30**, 37–60.

Meert JG and Lieberman BS (2008) The Neoproterozoic assembly of Gondwana and its relationship to the Ediacaran–Cambrian radiation. *Gondwana Research* **14**, 5–21.

Meschede M (1986) A method of discriminating between different types of mid-ocean ridge basalts and continental tholeiites with the Nb-Zr-Y diagram. *Chemical Geology* **56**, 207–18.

Mughal MS, Zhang C, Hussain A, Rehman HU, Du D and Hameed F (2022) Pre-Himalayan crustal growth in the Indian plate: implications from U-Pb dating, geochemical and Sr-Nd isotopic systematics. *Precambrian Research* **383**, 106920.

Mukherjee BK and Sachan HK (2001) Discovery of coesite from Indian Himalaya: a record of ultra-high pressure metamorphism in Indian Continental Crust. *Current Science* **81**, 1358–61.

O'Brien PJ (2019) Eclogites and other high-pressure rocks in the Himalaya: a review. *Geological Society, London, Special Publications* **483**, 183–213.

Ogasawara M, Fukuyama M, Siddiqui RH and Zhao Y (2019) Origin of the Ordovician Mansehra granite in the NW Himalaya, Pakistan: constraints from Sr–Nd isotopic data, zircon U–Pb age and Hf isotopes. *Geological Society, London, Special Publications* **481**, 277–98.

Oh CW, Imayama T, Jeon J and Yi K (2017) Regional Middle Paleozoic metamorphism in the southwestern Gyeonggi Massif, South Korea: its implications for tectonics in Northeast Asia. *Journal of Asian Earth Sciences* **145**, 542–64.

Pan R, Macris CA and Menold CA (2023) Fluid evolution during burial and exhumation of the Tso Morari UHP complex, NW India: constraints from mineralogy, geochemistry, and thermodynamic modeling. *Contributions to Mineralogy and Petrology* **178**, 3.

Pearce JA and Norry MJ (1979) Petrogenetic implications of Ti, Zr, Y, and Nb variations in volcanic rocks. *Contributions to Mineralogy and Petrology* **69**, 33–47.

Polat A and Hofmann AW (2003) Alteration and geochemical patterns in the 3.7–3.8 Ga Isua greenstone belt, West Greenland. *Precambrian Research* **126**, 197–218.

Qi L, Cawood PA, Xu Y, Du Y, Zhang H and Zhang Z (2020) Linking South China to North India from the late Tonian to Ediacaran: constraints from the Cathaysia Block. *Precambrian Research* **350**, 105898.

Rao DR and Rai H (2006) Signatures of rift environment in the production of garnet-amphibolites and eclogites from Tso-Morari region, Ladakh, India: a geochemical study. *Gondwana Research* **9**, 512–23.

Rehman HU (2019) Geochronological enigma of the HP–UHP rocks in the Himalayan orogen. *Geological Society, London, Special Publications* **474**, 183–207.

Rehman HU, Lee H-Y, Chung S-L, Khan T, O'Brien PJ and Yamamoto H (2016) Source and mode of the Permian Panjal Trap magmatism: evidence from zircon U–Pb and Hf isotopes and trace element data from the Himalayan ultrahigh-pressure rocks. *Lithos* **260**, 286–99.

Rudnick RL and Gao S (2003) 3.01 – composition of the continental crust. In *Treatise on Geochemistry* (eds HD Holland & KK Turekian), pp. 1–64. Oxford: Elsevier-Pergamon.

Salters VJM and Stracke A (2004) Composition of the depleted mantle. *Geochemistry, Geophysics, Geosystems* **5**, Q05B07.

Sen A, Sen K, Chatterjee A, Choudhary S and Dey A (2021) Understanding pre- and syn-orogenic tectonic evolution in western Himalaya through age and petrogenesis of Palaeozoic and Cenozoic granites from upper structural levels of Bhagirathi Valley, NW India. *Geological Magazine* **159**, 97–123.

Shao T, Xia Y, Ding X, Cai Y and Song M (2019) Zircon saturation in terrestrial basaltic melts and its geological implications. *Solid Earth Sciences* **4**, 27–42.

Shellnutt JG (2016) Igneous rock associations 21. The early Permian Panjal traps of the Western Himalaya. *Geoscience Canada* **43**, 251.

de Sigoyer J, Guillot S and Dick P (2004) Exhumation of the ultrahigh-pressure Tso Morari unit in eastern Ladakh (NW Himalaya): a case study. *Tectonics* **23**, 1–18.

Song S, Bi H, Qi S, Yang L, Allen MB, Niu Y, Su L and Li W (2018) HP–UHP metamorphic belt in the East Kunlun Orogen: final closure of the Proto-Tethys ocean and formation of the Pan-North-China continent. *Journal of Petrology* **59**, 2043–60.

Spencer DA, Tonarini S and Pognante U (1995) Geochemical and Sr-Nd isotopic characterisation of Higher Himalayan eclogites (and associated metabasites). *European Journal of Mineralogy*, **7**, 89–102.

St-Onge MR, Rayner N, Palin RM, Searle MP and Waters DJ (2013) Integrated pressure-temperature-time constraints for the Tso Morari dome (Northwest India): implications for the burial and exhumation path of UHP units in the western Himalaya. *Journal of Metamorphic Geology* **31**, 469–504.

Sun S-S and McDonough WF (1989) Chemical and isotopic systematics of ocean basalt: implications for mantle composition and processes. *Geological Society Special Publication* **42**, 323–45.

Trivedi JR, Sharma KK and Gopalan K (1986) Widespread Caledonian magmatism in Himalaya and its tectonic significance. *Terra Cognita* **6**, 144.

Wang Y-H, Zhang L-F, Li S-Z and Somerville I (2017) Zircon U–Pb dating and phase equilibria modelling of gneisses from Dinggye area, Ama Drime Massif, central Himalaya. *Geological Journal* **52**(S1), 476–94.

Wedepohl KH (1995) The composition of the continental crust. *Geochimica et Cosmochimica Acta* **59**, 1217–32.

Whitney DL and Evans BW (2010) Abbreviations for names of rock-forming minerals. *American Mineralogist* **95**, 185–7.

Wilson M (1989). *Igneous Petrogenesis*. London: Unwin Hyman, 464 pp.

Xia L and Li X (2019) Basalt geochemistry as a diagnostic indicator of tectonic setting. *Gondwana Research* **65**, 43–67.

Yang J, Xu Z, Li Z, Xu X, Li T, Ren Y, Li H, Chen S and Robinson PT (2009) Discovery of an eclogite belt in the Lhasa block, Tibet: a new border for Paleo-Tethys? *Journal of Asian Earth Sciences* **34**, 76–89.

Zhang G, Wang J, Webb AAG, Zhang L, Liu S, Fu B, Wu C and Wang S (2022) The protoliths of central Himalayan eclogites. *GSA Bulletin* **134**, 1949–66.

Zhang J, Meng F and Yang J (2005) A new HP/LT metamorphic Terrane in the Northern Altyn Tagh, Western China. *International Geology Review* **47**, 371–86.

Zhang ZM, Dong X, Santosh M and Zhao GC (2014) Metamorphism and tectonic evolution of the Lhasa terrane, Central Tibet. *Gondwana Research* **25**, 170–89.